- $_{\rm 1}$ $\,$ International Journal of Computational Geometry & Applications
- 2 © World Scientific Publishing Company

On the Reconstruction of Geodesic Subspaces of \mathbb{R}^N

Brittany Terese Fasy

5	School of Computing $m{arepsilon}$ Dept. Mathematical Sciences, Montana State University
6	$Bozeman,\ MT\ 59717\ USA$
7	brittany.fasy@montana.edu
8	Rafal Komendarczyk
9	Mathematics, Tulane University
10	New Orleans, LA 70118 USA
11	rako @tulane.edu
12	Sushovan Majhi*
13	School of Information, University of California
14	Berkeley, CA 94720 USA
15	smajhi@berkeley.edu
16	Carola Wenk
17	Computer Science, Tulane University
18	New Orleans, LA 70118 USA
19	cwenk@tulane.edu
20	Received (received date)
21	Revised (revised date)
22	Communicated by (Name)
23	ABSTRACT
24	We consider the topological and geometric reconstruction of a geodesic subspace of \mathbb{R}^N both from
25	the Čech and Vietoris-Rips filtrations on a finite, Hausdorff-close, Euclidean sample. Our recon-
26	struction technique leverages the intrinsic length metric induced by the geodesics on the subspace
27	We consider the distortion and convexity radius as our sampling parameters for the reconstruc-
28	tion problem. For a geodesic subspace with finite distortion and positive convexity radius, we
29	guarantee a correct computation of its homotopy and homology groups from the sample. This
30	technique provides alternative sampling conditions to the existing and commonly used conditions
31	based on weak feature size and μ -reach, and performs better under certain types of perturbations
32	of the geodesic subspace. For geodesic subspaces of \mathbb{R}^2 , we also devise an algorithm to output a
33 34	homotopy equivalent geometric complex that has a very small Hausdorff distance to the unknown underlying space.
35	Keywords: Vietoris-Rips complex, Geodesic spaces, Shape reconstruction, Map construction

^{*}Corresponding author

1. Introduction

50

51

52

53

54

55

56

57

60

61

62

63

64

65

66

67

71

72

73

75

With the advent of modern sampling technologies, such as GPS, sensors, medical imaging, etc., Euclidean point-clouds are becoming widely available for analysis. In the last 38 decade, the problem of reconstructing an (unknown) Euclidean shape, from a (noisy) sam-39 ple around it, has received a far and wide attention both in theoretical and applied literature; 40 see [1, 2, 3, 4, 5, 6]. The nature of such a reconstruction attempt can commonly be classi-41 fied as being topological or geometric. A topological reconstruction is usually attributed to 42 inferring significant topological features—such as homology and homotopy groups—of the 43 hidden shape of interest. To be more specific, one may also say homological reconstruction or 44 homotopy type reconstruction. A much stronger paradigm is the geometric reconstruction, 45 where one is interested in producing, from the sample, a Euclidean subset that is homotopy equivalent and geometrically "close" (e.g., in Hausdorff distance) to the underlying shape.

The nature of the problem and the techniques of the solution change depending on the type of the shape X and the sample S considered, as well as how their "closeness" is measured. The most natural distance measure between two abstract metric spaces is the Gromov-Hausdorff distance, which measures how "metrically close" two metric spaces are. The reconstruction of a geodesic metric space X from another metric space S that is Gromov-Hausdorff close to S is considered in [7, 8]. For a Euclidean shape S and a Euclidean sample S, however, the sample density is usually quantified by their Hausdorff distance. For the Hausdorff-type reconstruction of Euclidean shapes, see [3, 5, 6, 4].

In many applications, a point cloud approximates a geodesic subspace (see Definition 2.1) of Euclidean space. Examples include GPS trajectories sampled around a road-network (modeled as sampling paths in a graph in \mathbb{R}^2), earthquake data sampled around the filamentary trajectory of the shock, or 3D medical imaging. The intrinsic geodesics of these underlying shapes enjoy a rich geometric structure. Capturing that structure from the sampled data is the challenge. The length metric d_L (see (1)) turns them into geodesic subspaces of \mathbb{R}^N . In this work, we consider both topological and geometric reconstruction of a geodesic subspace X of \mathbb{R}^N from a finite Hausdorff-close Euclidean sample.

In shape reconstruction, the use of various simplicial complexes built on the point-clouds is becoming increasingly popular; see for example [9, 10, 11, 5, 12]. The most common of them are Vietoris-Rips and Čech complexes. In this work, we use filtrations of both of them, and we recognize the distortion $\delta = \delta(X)$ and convexity radius $\rho = \rho(X)$ of X to be natural sampling parameters when the geodesic subspaces of \mathbb{R}^N are considered; see Section 2 for their formal definitions.

Our homological reconstruction approach is similar to [5], which is based on the weak feature size (wfs) of the underlying space. However, the use of partition of unity, for example, in the proof of Theorem 3.10 makes our techniques substantially different. The novelty of this paper is discerned by the introduction of distortion and convexity radius as sampling parameters, which is not related to the known sampling parameters such as the reach, μ -reach or wfs [6, 4, 10]. These works are based on an analysis of the gradient flow of the Euclidean distance function to X in \mathbb{R}^N and its critical points. Our techniques are substantially different from that and our results apply to a large class of spaces including smooth

submanifolds of \mathbb{R}^N , finite embedded graphs and higher dimensional simplicial complexes.

- As an application of our reconstruction technique, we develop in Section 4 a new topological
- approach for the reconstruction of embedded graphs.

1.1. Review of Related Works

91

92

93

100

101

102

103

104

105

106

107

108

110

111

112

113

114

115

116

This subsection surveys relevant and pivotal results in shape reconstruction from point clouds using topological methods, and compares them to the results of this paper. Table 1 presents a list of some of the most related results alongside the contribution presented in this work. For necessary definitions and background we refer the reader to Section 2.

Reach. The most well-behaved spaces are smooth Euclidean submanifolds, more generally spaces with a positive $\operatorname{reach} r(X)$. In [3], the authors apply geometric and topological tools to reconstruct a smooth submanifold by the union of Euclidean balls of sufficiently small radius around a dense subset. The work uses the reach of the embedded submanifold as the sampling parameter. In a more recent work ([15]), the authors improve some of the previously known bounds and develop homotopy-type reconstruction of a Euclidean (compact) subset with positive reach (and μ -reach) using Čech and Vietoris-Rips complexes on a sample.

The above results do not apply when considering shapes beyond the class of Euclidean submanifolds or spaces that do not have a positive reach, although such shapes are frequently encountered in practical applications. A common reason for a space to have a vanishing reach is the presence of sharp corners and branchings. Such spaces include graphs, embedded simplicial complexes, manifolds with corners—also the type of shapes we consider in this work for reconstruction. For manifold reconstruction by Vietoris-Rips complexes in a slightly different but related context, see [11, 16].

Weak Feature Size, μ -Reach. In developing a sampling theory for general compact sets in \mathbb{R}^N , the notion of weak feature size (wfs) was introduced in [4] as the infimum of the positive critical values of the distance function to the compact set. Using the wfs as a sampling condition, the authors developed a persistence-based approach to reconstruct the homology groups and the fundamental group of a hidden shape from the Euclidean thickenings of the sample around it.

The results have been further extended in [5] to facilitate reconstruction of homology groups from Čech, Vietoris-Rips, and witness complexes built on the sample. In comparison with the manifold reconstruction result in [3], the techniques of [4, 5] apply to much less regular subspaces of \mathbb{R}^N , such as compact Euclidean neighborhood retracts [17, 18]—as long as they have a positive wfs.

The notion of the wfs of a Euclidean compact set was generalized in [6] by introducing the concept of μ -reach, denoted $r_{\mu}(X)$. A homotopy-type reconstruction of spaces with positive μ -reach has been developed in [6, 10]. Although these works consider for reconstruction spaces beyond the class of positive wfs, the difficulty lies in applying the results to shapes as simple as an embedded tree. Also, choosing a suitable μ so that the μ -reach is positive is not always clear.

Table 1: Reconstruction results. Parameters (params.) are: weak feature size (wfs), μ -reach (R), shorted edge length (b), global reach (ξ), smallest turning angle (α), distortion (δ), and convexity radius (ρ).

Authors	Space X	Param.	Condition on S	Result
Niyogi et al. [3]	manifolds	ξ	$\varepsilon < \sqrt{\frac{3}{5}}\xi$ and $S \subset X$ is $\frac{\varepsilon}{2}$ -dense	S^{ε} deformation retracts to X
Chazal, Lieutier [4]	compact sets	wfs	$d_H(X,S) < \varepsilon < \frac{\operatorname{wfs}(X)}{4}$	$Im(i_*) \simeq H_*(X^{\alpha})$, where $i: S^{\varepsilon} \to S^{3\varepsilon}$ and α is sufficiently small
Chazal, Oudot [5]	compact sets	wfs		$Im(i_*) \simeq H_*(X^{\alpha})$, where $i: \mathcal{R}_{\varepsilon}(S) \to \mathcal{R}_{4\varepsilon}(S)$, α is sufficiently small
Attali et al. [10]	compact sets	μ -reach R	$d_H(X,S) \le \varepsilon < \lambda^{\operatorname{cech}}(\mu)R$	$\mathcal{C}_{\alpha}(S)$ is homotopy equivalent to X^{η} for $\eta \in (0, R)$
Anjaneya et al. [13]	abstract metric graphs	b, r	$S \text{ is an } \\ (\varepsilon, R) \text{-approximation,} \\ \frac{15\varepsilon}{2} < b < \min\left\{\frac{R}{4}, \frac{3b - 6\varepsilon}{5}\right\}$	homeomorphic graph
Wasserman et al. [14]	embedded metric graphs	μ of each edge, ξ , α , b , τ	$S \text{ is } \frac{\delta}{2}\text{-dense in} $ $X^{\alpha}, \ 0 < r + \delta < \xi - 2\sigma, $ and $0 < \delta < f(b, \alpha, \tau, \xi, \sigma)$	isomorphic pseudo-graph
Theorem 3.5	geodesic spaces	δ, ho	$d_H(X,S) < \frac{\varepsilon}{4} < \frac{\rho}{2\delta(3\delta+2)}$	$Im(i_*) \simeq H_*(X)$, where $i:$ $\mathcal{R}_{\varepsilon}(S) \to \mathcal{R}_{\frac{1}{2}(3\delta+1)\varepsilon}(S)$
Theorem 4.7	planar subspaces	δ, ho	$d_H(X,S) < \frac{\varepsilon}{3} < \frac{\rho}{\delta(15\delta+2)}$	Hausdorff-close, homotopy equivalent subset

Our topological reconstruction results (Theorem 3.5 and Theorem 3.10), are very similar in style to the results presented in [5]. However, the use of partition of unity for Čech complexes and homotopy equivalence result of Hausmann ([19]) for Vietoris-Rips complexes make our proofs very different. The wfs-based technique employed in [4, 5] restricts their results to work for homology with coefficients only in a field. Moreover, it's not apparently

123

124

125

126

127

129

130

131

132

133

134

135

136

137

138

139

140

141

142

144

145

146

147

148

149

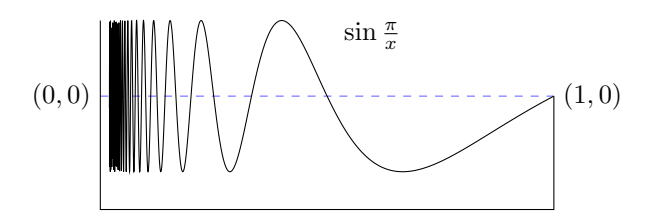


Fig. 1: The compact set X (Warsaw circle) has a positive wfs, but X and X^{λ} do not have the same homotopy type for any $\lambda > 0$. In fact, X has the weak homotopy type of a point, whereas X^{λ} has the homotopy type of S^1 .

clear whether the results can easily be extended to higher homotopy groups. Our reconstruction results, however, do not suffer such restrictions; see Remark 3.11.

Apart from the fact that we employ $\delta(X)$ and $\rho(X)$ for our sampling condition, all wfs (and μ -reach) based results guarantee a reconstruction of a thickening X^{λ} of X and not X directly. There are known pathological examples of spaces where the thickening (however small) is not homotopy equivalent to the underlying space, such as the Warsaw circle shown in Figure 1. Although the homological reconstruction results in our work concern the homological reconstruction of the subspace X itself, not the thickening of X, they are not strong enough to apply in the case of the Warsaw circle because of $\delta(X) = +\infty$ in this case.

Another notable difference in the previously discussed approaches appears in the cases where X is "slightly perturbed", e.g., a submanifold with corners. Such a perturbation is illustrated in Figure 2 for a circle X topologically embedded^a in \mathbb{R}^2 . The top part of the space X is the graph of a rectifiable curve $\gamma:[0,1]\to\mathbb{R}^2$ such that, when restricted to the segment $\left\lceil \frac{1}{n+1}, \frac{1}{n} \right\rceil$, it is a half-circle of diameter $\frac{1}{n(n+1)}$ for n odd and a line-segment for n even. For this space, the set of critical points of the distance function is an infinite set with an accumulation point at (0,0). Consequently, wfs(X) = 0. However, X has a finite distortion $\delta = \frac{\pi}{2}$ and a positive intrinsic convexity radius: $\rho(X) > 0$. Thus X fails to satisfy the conditions of the reconstruction results of [4, 5], however our results apply to this case. Another important point, suggested by the example of Figure 2, is that any embedded submanifold X in \mathbb{R}^N can be perturbed to a submanifold X', just by adding a small "spherical cap" at any of its points. Such a small perturbation does not change the distortion and the convexity radius too much, however can produce very small wfs, because we introduce a critical point of the distance function at the center of the cap. Small values of wfs result in large sample sizes needed for the reconstruction.

Metric Graph Reconstruction. We finish this introduction with a quick summary of some of the existing works on reconstruction of embedded metric graphs ([13, 20, 8]). In [13], the authors consider an abstract metric graph and a sample that is close to it in Gromov-Hausdorff metric, and reconstruct the structure of the metric graph along with the metric

^aa topological embedding is simply a C^0 -embedding.

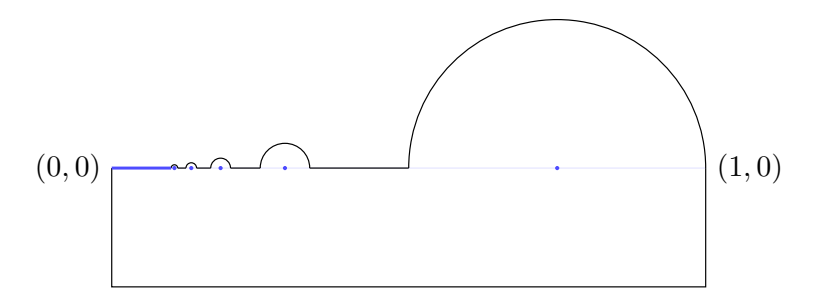


Fig. 2: The space X is a compact Euclidean subspace with $\mathsf{wfs}(X) = 0$ and $\mathsf{r}_{\mu}(X) = 0$. The critical points of the distance function are shown in blue; they accumulate at (0,0). However, X has a finite distortion and a positive convexity radius.

on it. In a more recent work [20], the authors show a statistical treatment of metric graph reconstruction. They consider an embedded metric graph and a Euclidean sample around it. The Gromov-Hausdorff proximity used in [13] is replaced by the density assumption. The algorithm presented in [13] only reconstructs the connectivity of the vertices of the underlying metric graph and outputs an isomorphic pseudo-graph. And lastly, we mention that the first Betti number of an abstract metric graph is computed by considering the persistent cycles in the Vietoris-Rips complexes of a sample that is very close to it, with respect to the Gromov-Hausdorff distance; see [8, Lemma 6.1]. In Gromov-Hausdorff type reconstruction schemes, a small Gromov-Hausdorff distance between the graph and the sample guarantees a successful reconstruction. These methods are not a good choice when embedded graphs in \mathbb{R}^N are considered. For an embedded graph with the induced length metric and a Euclidean sample around it, the Gromov-Hausdorff distance is not guaranteed to be made infinitely small, even if a dense enough sample is taken. Also, most of the above mentioned works may be insufficient to give a geometrically close embedding for the reconstruction. Whereas our technique, presented in Section 4, can successfully be used to reconstruct embedded graphs; see Corollary 4.8.

1.2. Our Contribution

150

151

152

153

155

156

157

158

159

160

161

162

163

165

166

167

168

170

171

172

173

174

175

176

177

One of the major contributions of this work is to reconstruct geodesic subspaces of \mathbb{R}^N , both topologically and geometrically. In our pursuit, we recognize distortion and convexity radius as new sampling parameters. These sampling parameters are very natural properties of geodesic spaces.

In Section 2, along with the other important notions of metric geometry and algebraic topology that we use throughout this paper, we define convexity radius and distortion of a geodesic space.

In Section 3, our main topological reconstruction results for a geodesic subspace X of \mathbb{R}^N are presented. When the distortion is finite and the convexity radius is positive, the Vietoris-Rips and Čech filtrations of the sample are shown to successfully compute the homology and homotopy groups of X (Theorem 3.5 and Theorem 3.10).

179

180

181

182

183

184

185

186

196

198

199

201

202

203

In Section 4, we consider geometric reconstruction of geodesic subspaces. We construct a complex on the sample as our geometric reconstruction of the space of interest. Theorem 4.3 establishes the isomorphism of their fundamental groups. As an interesting application in Section 4.2, we consider the geometric reconstruction of planar subspaces and embedded planar graphs (Definition 4.4) in particular. In Theorem 4.7, we compute a homotopy equivalent geometric complex in the same ambient space that is also Hausdorff-close to X. Since the sample S can be taken to be finite, our result gives rise to an efficient algorithm (Algorithm 1) for the geometric reconstruction of planar embedded graphs.

2. Notation and Background

In this section, we provide a brief overview of useful notation and classical results from metric 187 geometry and algebraic topology. For more detailed and complete treatment, we refer the 188 reader to textbooks on metric geometry [21, 22] and algebraic topology [23, 24, 25].

2.1. Geodesic Subspaces, Distortion, Convexity Radius

We first present relevant definitions from metric geometry.

Geodesic Subspaces (of \mathbb{R}^N) We start with the unit interval $I := [0,1] \subset \mathbb{R}$. A continuous function $\gamma \colon I \to \mathbb{R}^N$ is called a path. We call $T = \{t_i\}_{i=0}^k$ a discretization of Iif $0 = t_0 < t_1 < t_2 < \ldots < t_k = 1$. We create a piecewise linear path by using straight line segments to connect $\gamma(t_i)$ with $\gamma(t_{i+1})$ for each $i \in \{0, 1, \dots, k-1\}$. We often equip \mathbb{R}^N with the Euclidean, or L_2 distance, $d_2 : \mathbb{R}^N \times \mathbb{R}^N \to \mathbb{R}$ defined by $d_2(x,y) := ||x-y||_2$. Let $\gamma \colon I \to \mathbb{R}^N$ be a (continuous) path. The *length* of γ is defined as:

$$L(\gamma) := \sup_{T} \sum_{i \in \{1, 2, \dots, |T|\}} d_2 \left(\gamma(t_i), \gamma(t_{i+1}) \right),$$

where the supremum is taken over all finite discretizations of I. Furthermore, the curve γ is called rectifiable if $L(\gamma)$ is finite. For a path-connected subset $X \subseteq \mathbb{R}^N$, we call the restriction of d_2 to X the restricted metric on X. We define the induced length metric or geodesic metric, $d_L: X \times X \to R$, by 195

$$d_L(x,y) = \inf_{\gamma:[0,1] \to X} L(\gamma), \tag{1}$$

where the infimum is taken over all paths $\gamma: I \to X$ such that $\gamma(0) = x$ and $\gamma(1) = y$.

Definition 2.1 (Geodesic Subspace). We call $X \subseteq \mathbb{R}^N$ a geodesic subspace if between any pair of points $x, y \in X$, there exists a rectifiable path on X starting at x and ending at y whose length is $d_L(x, y)$.

One example of a geodesic subspace is a connected and compact subset of \mathbb{R}^N . The "niceness" of an geodesic subspace is quantified by its distortion, a concept first introduced by M. Gromov in the context of knots on Riemannian manifolds [26, 27, 22]. For a geodesic subspace $X \subseteq \mathbb{R}^N$, we consider the map $f:(X,d_2)\to (X,d_L)$ induced by the identity map

207

208

209

211

212

213

214

215

216

217

218

219

220

221

on X. The distortion of X is the best Lipschitz constant for f. More formally, we have the following definition.

Definition 2.2 (Distortion). The distortion of the induced length metric d_L with respect to Euclidean distance over a set $X \subseteq \mathbb{R}^N$ is defined as:

$$\delta := \delta(X) = \sup_{x \neq y \in X} \frac{d_L(x, y)}{\|x - y\|_2}.$$

For simplicity of exposition, we refer to δ as the distortion of X.

Since d_L is the induced length metric, δ is bounded below by one and above by $+\infty$. If X is a straight line segment, then $\delta = 1$. On the other extreme, if X is the subspace $\{(x,y) \in \mathbb{R}^2 \mid x^2 = y^3\}$, then $\delta = +\infty$. To see this, consider the limit as ε approaches zero of the two points $(-\varepsilon^{3/2}, \varepsilon) \in X$ and $(\varepsilon^{3/2}, \varepsilon) \in X$, getting arbitrarily close to the cusp point (0,0). Thus, both the lower and upper bounds on δ are tight. For more on distortion, see [28].

Remark 2.3 (Equivalence of Topologies). Given a metric space (X,d), we can topologize X with metric balls; that is, the topology is generated by sets of the form $B_d(x,r) := \{y \in X \mid d(x,y) < r\}$, where $x \in X$ and $r \in \mathbb{R}$. If we assume that d_L has finite distortion with respect to d_2 , then (X,d_L) and (X,d_2) have equivalent topologies. The equivalence of the two topologies is a direct consequence of the following inequalities for $x, y \in X$:

$$||x - y||_2 \le d_L(x, y) \le \delta ||x - y||_2.$$
 (2)

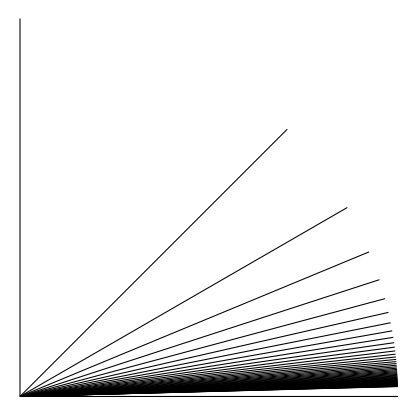


Fig. 3: The set X, the closure of the union of the falling segments in the figure, is known as the *infinite broom*. The topology of (X, d_2) is strictly finer than the length metric topology of (X, d_L) . The latter topology is locally path-connected; whereas, the former topology is not.

Equivalence of the topologies does not generally hold if the distortion of X is not finite. For an example, let $X \subset \mathbb{R}^2$ be the closure of the union of line segments $\left\{\left[(0,0),\left(\cos\frac{\pi}{2i},\sin\frac{\pi}{2i}\right)\right]\right\}_{i\in\mathbb{N}}$, as shown in Figure 3. Such a space is also known as

228

229

243

244

250

251

252

253

254

255

256

the infinite broom. We see that the distortion of the space is infinite by considering the sequence $a_i = (\cos \frac{\pi}{2i}, \sin \frac{\pi}{2i})$ of points on the right end of the spokes of the broom:

$$\lim_{i \to \infty} \frac{d_L((0,1), a_i)}{\|(0,1) - a_i\|_2} = \infty.$$

The Euclidean metric topology, in this case, is strictly finer than the length metric topology, as (X, d_L) is locally path-connected, but (X, d_2) is not.

Convexity Radius Convexity radius of the underlying geodesic subspace is one of the 230 parameters of X used in all our reconstruction results. We start with its formal definition 231 from [19]. Although the concept is defined for general length spaces, we restrict ourselves 232 to only geodesic subspaces. 233

Definition 2.4 (Convexity Radius). We define the *convexity radius*, denoted ρ , of a geodesic subspace $X \subseteq \mathbb{R}^N$ to be the supremum of all r > 0 such that: 235

- (1) For all $x, y \in X$ with $d_L(x, y) < 2r$, there exists a unique (length-minimizing) geodesic 236 path joining x and y. 237
- (2) If $x, y, z, u \in X$ such that $d_L(x, y) < r$, $d_L(y, z) < r$, $d_L(z, x)$ 238 and u is a point on the (length-minimizing) geodesic path joining x and y. then $d_L(u, z) \leq \max\{d_L(x, z), d_L(y, z)\}.$
- If γ and γ' are arc-length parametrized (length-minimizing) geodesics on X such that $\gamma(0) = \gamma'(0)$, then $d_L(\gamma(ts), \gamma'(ts')) \leq d_L(\gamma(s), \gamma'(s'))$ for $0 \leq s, s' < r$ and $0 \leq t \leq 1$. 242

Consider a circle in \mathbb{R}^2 with perimeter R; its convexity radius is $\frac{R}{4}$. Also, the convexity radius of an embedded graph is $\frac{b}{4}$, where b is the length of its smallest simple cycle. It is well-known that the convexity radius of a compact Riemannian manifold is positive. The convexity radius of a geodesic space is an intrinsic property.

2.2. Simplicial Complexes, Nerve Lemma

We finally conclude this section by outlining a few important notions from algebraic topol-248 ogy. Readers are referred to [23, 24, 25] for more details. 249

Abstract Simplicial Complex The combinatorial analogue of a topological space, often used in algebraic and combinatorial topology, is an abstract simplicial complex. An abstract simplicial complex K is a collection of finite sets such that if $\sigma \in K$, then so are all its non-empty subsets.

In general, elements of K are called *simplices* of K. The singleton sets in K are often called the vertices of K. If a simplex $\sigma \in K$ has cardinality (q+1), then it is called a q-simplex (or the dimension of σ is q or dim $(\sigma) = q$). If $\sigma' \subseteq \sigma$, then σ' is called a face of σ .

Simplicial Maps and Contiguity Let K_1 and K_2 be abstract simplicial complexes with vertex sets \mathcal{V}_1 and \mathcal{V}_2 , respectively. A vertex map is a map between the vertex sets. Let $\phi: \mathcal{V}_1 \to \mathcal{V}_2$ be a vertex map. If, for all $\sigma \in \mathcal{K}_1$, we have $\phi(\sigma) := \bigcup_{v \in \sigma} \{\phi(v)\}$ is,

in fact, an element of \mathcal{K}_2 , then we say that ϕ induces a *simplicial map* $\phi: \mathcal{K}_1 \to \mathcal{K}_2$.

Two simplicial maps $\phi_1, \phi_2: \mathcal{K}_1 \to \mathcal{K}_2$ are called *contiguous* if for every simplex $\sigma_1 \in \mathcal{K}_1$, there exists $\sigma_2 \in \mathcal{K}_2$ such that $\phi_1(\sigma_1) \cup \phi_2(\sigma_1) \subseteq \sigma_2$. A simplicial map between abstract simplicial complexes is the combinatorial analogue of a continuous map between topological spaces; likewise, contiguous simplicial maps play the role of homotopic maps in the combinatorial world.

Geometric Complex Although, abstract simplicial complexes have enough combinatorial structure to define simplicial homology and homotopy, they are not topological spaces. For an abstract simplicial complex \mathcal{K} with vertex set \mathcal{V} , its underlying topological space or geometric complex, denoted as $|\mathcal{K}|$, is defined as the space of all functions $\alpha: \mathcal{V} \to [0,1]$, also called barycentric coordinates, satisfying the following two properties:

271 (1) supp
$$(\alpha) := \{v \in \mathcal{V} \mid \alpha(v) \neq 0\} \in \mathcal{K}$$
272 (2) $\sum_{v \in \mathcal{V}} \alpha(v) = 1$.

276

292

The details on the topologies on $|\mathcal{K}|$ and their relations can be found in [24, 25]. In this work, we use the standard *metric topology* on $|\mathcal{K}|$, as defined in [25]. Naturally, a simplicial map $\phi : \mathcal{K}_1 \to \mathcal{K}_2$ induces a continuous map $|\phi| : |\mathcal{K}_1| \to |\mathcal{K}_2|$ defined by

$$|\phi|(\alpha)(v') = \sum_{\phi(v)=v'} \alpha(v), \text{ for } v' \in \mathcal{K}_2.$$

As one expects, the contiguous simplicial maps induce homotopic continuous maps between their respective underlying topological spaces; see [25] for a proof.

Nerve Lemma A critical ingredient for our Čech reconstruction results is the Nerve Lemma or a modification thereof; therefore, we discuss the concept here. An open cover $\mathcal{U} = \{U_i\}_{i \in \Lambda}$ of a topological space X is called a *good cover* if all finite intersections of its elements are contractible. The *nerve* of \mathcal{U} , denoted $\mathcal{N}(\mathcal{U})$, is defined to be the simplicial complex having Λ as its vertex set, and for each non-empty k-way intersection $U_{i_1} \cap U_{i_2} \cap \ldots \cap U_{i_k}$, the subset $\{i_1, i_2, \ldots, i_k\}$ is a simplex of $\mathcal{N}(\mathcal{U})$. Under the right assumptions, the nerve preserves the homotopy type of the union X, as stated by the following fundamental result.

Lemma 2.5 (Nerve Lemma [29]). Let $\mathcal{U} = \{U_i\}_{i \in \Lambda}$ be a good open cover of a topological space X. Then, the underlying topological space $|\mathcal{N}(\mathcal{U})|$ is homotopy equivalent to X.

Remark 2.6. If the open cover \mathcal{U} is locally finite, then the homotopy equivalence in the Nerve Lemma is usually constructed with the help of a partition of unity for the cover [23]. Specifically, let $h: X \longrightarrow |\mathcal{N}(\mathcal{U})|$ be a homotopy equivalence. Then, a partition of unity is a collection of continuous functions $\{\varphi_i: X \longrightarrow [0,1]\}_{i \in \Lambda}$ such that for all $x \in X$,

$$h(x) = \sum_{i \in \Lambda} \varphi_i(x) v_i, \tag{3}$$

where v_i denotes the vertex of $\mathcal{N}(\mathcal{U})$ corresponding to the cover element U_i . In addition, each φ_i must satisfy the following two requirements: (i) for all $i \in \Lambda$, the support of φ_i ,

299

300

301

302

303

304

305

306

310

311

312

324

denoted **supp** (φ_i) , is a compact proper subset of U_i , and (ii) for all $x \in X$, $\sum_{i \in \Lambda} \varphi_i(x) = 1$.

Čech and Vietoris-Rips Complexes Consider a subspace A of a metric space (M,d) and a positive scale α . The nerve of the collection of open metric balls of radius α centered at the points of A is known as the $\check{C}ech$ complex of A at scale (radius) α . We are interested in $\check{C}ech$ complexes in two metric spaces: Euclidean and the length metric space. Let $X \subseteq \mathbb{R}^N$. Then, the Čech complex under the standard Euclidean metric is: $\mathcal{C}_{\alpha}(X) := \mathcal{N}(\{\mathbb{B}(x,r)\}_{x \in X}),$ where $\mathbb{B}(x,r)$ is the Euclidean ball of radius r centered at x. The Čech complex under the length metric (X, d_L) is $\mathcal{C}^L_{\alpha}(A) := \mathcal{N}(\{\mathbb{B}^L(x, r)\}_{x \in X})$, where $\mathbb{B}^L(x, r)$ denotes the metric ball of radius r centered at X in (X, d_L) . Note that these complexes may be infinite.

The Vietoris-Rips Complex is an abstract simplicial complex having a k-simplex for every set of (k+1) points in A of diameter at most α . Explicit knowledge about the entire metric space (M,d) is not needed to compute the complex. Unlike the Čech complex, the Vietoris-Rips complex is completely determined by the restriction of the metric to the subset A. For $X \subseteq \mathbb{R}^N$ under the standard Euclidean metric, we denote it simply by $\mathcal{R}_{\alpha}(X)$. In the case when $A \subseteq X$ equipped with length metric (X, d_L) , we denote the Vietoris-Rips complex by $\mathcal{R}_{\alpha}^{L}(A)$.

Together, the definition of convexity radius and Nerve Lemma immediately imply the following fact:

Lemma 2.7 (Čech Equivalence). Let $X \subseteq \mathbb{R}^N$ be a geodesic subspace with a positive 313 convexity radius ρ , and let $0 < \varepsilon < \rho$. Let A be an ε -dense subset of X with respect to the d_L 314 metric. Then, the complex $\mathcal{C}_{\varepsilon}^{L}(A)$ is homotopy equivalent to X. 315

Proof. Since A is an ε -dense subset of X, we know that $\mathcal{U} := \bigcup_{a \in A} \mathbb{B}^L(a, \varepsilon)$ is an open cover 316 of (X, d_L) . Since $\varepsilon < \rho$ and by the definition of convexity radius (Definition 2.4), we know 317 that for each $x \in X$ and $y \in \mathbb{B}^{L}(x,\varepsilon)$, there exists a unique length-minimizing geodesic 318 path between x and y. Using these paths to define a deformation retract from $\mathbb{B}^L(x,\varepsilon)$ 319 to x, we conclude that the metric balls in \mathcal{U} are contractible. Since any finite intersection of 320 metric balls in \mathcal{U} has dimeter less than 2ε , by the similar argument it is also contractible. Hence, \mathcal{U} is a good cover of X. By the Nerve Lemma (Lemma 2.5), we conclude that the complex $\mathcal{C}_{\varepsilon}^{L}(A)$ is homotopy equivalent to X. 323

3. Topological Reconstruction

In this section, we consider the problem of topological reconstruction of a geodesic subspace X of \mathbb{R}^N from a noisy sample S. From now on, unless otherwise stated, we assume that the underlying shape X has a positive convexity radius and a finite distortion, also that the sample S is a finite subset of \mathbb{R}^N . We show that both Čech and Vietoris-Rips 328 filtrations of S can be used to compute the homology and homotopy groups of X. Before we treat each type of complex separately, we show how the Čech and Vietoris-Rips complexes 330 behave under Hausdorff perturbation. 331

Lemma 3.1 (Hausdorff Distance and Complexes). Let $A, B \subseteq \mathbb{R}^N$ be finite, and ε be

a positive number such that $d_H(A,B) < \varepsilon$. Then for any $\alpha > 0$, there exist simplicial maps

$$\mathcal{C}_{\alpha}(A) \longrightarrow \mathcal{C}_{\alpha+\varepsilon}(B)$$

335 and

334

336

340

341

342

343

357

$$\mathcal{R}_{\alpha}(A) \longrightarrow \mathcal{R}_{\alpha+2\varepsilon}(B)$$

induced by a vertex map $\xi: A \to B$ such that for every vertex $a \in A$, we have $\|a - \xi(a)\|_2 < \varepsilon$. Moreover, such simplicial maps are unique, up to contiguity.

Proof. We first note the definition

$$d_H(A, B) = \inf \{ \varepsilon > 0 \mid A \subseteq B^{\varepsilon}, B \subseteq A^{\varepsilon} \},$$

where A^{ε} denotes the Euclidean thickening of A.

The definition of Hausdorff distance implies that if $d_H(A,B) < \varepsilon$, there exists a (possibly non-unique, non-continuous) map $\xi : A \to B$ such that $||a - \xi(a)||_2 < \varepsilon$. We show that this vertex map extends to a simplicial map between both Čech and Vietoris-Rips complexes.

Let $\sigma = \{a_0, a_1, \dots, a_k\}$ be a k-simplex of $\mathcal{C}_{\alpha}(A)$. By definition, there exists a point z in \mathbb{R}^N such that $||a_i - z||_2 < \alpha$ for all $i \in \{0, 1, \dots, k\}$. By the triangle inequality, we then have

$$\|\xi(a_i) - z\|_2 \le \|\xi(a_i) - a_i\|_2 + \|a_i - z\|_2 < \varepsilon + \alpha.$$

So, $\{\xi(a_0), \dots, \xi(a_k)\}$ is a simplex of $\mathcal{C}_{\alpha+\varepsilon}(B)$. Hence, ξ extends to a simplicial map between the Čech complexes. To argue for the uniqueness of the simplicial map, let us assume that η is another simplicial map with the property that for every vertex $a \in A$, we have $\|a-\eta(a)\|_2 < \varepsilon$. Again from the triangle inequality, we have $\|\eta(a_i)-z\|_2 < \varepsilon + \alpha$. So, $\xi(\sigma) \cup \eta(\sigma)$ is a simplex of $\mathcal{C}_{\alpha+\varepsilon}(B)$. Hence, ξ and η are contiguous.

For the Vietoris-Rips complex part, we follow a similar argument. Let $\sigma = \{a_0, a_1, \ldots, a_k\}$ be a k-simplex of $\mathcal{R}_{\alpha}(A)$. By definition, the diameter of σ is not greater than α . From the triangle inequality, we have

$$\|\xi(a_i) - \xi(a_j)\|_2 \le \|\xi(a_i) - a_i\|_2 + \|a_i - a_j\|_2 + \|\xi(a_j) - a_j\|_2 < 2\varepsilon + \alpha.$$

So, $\{\xi(a_0), \dots, \xi(a_k)\}$ is a simplex of $\mathcal{R}_{\alpha+2\varepsilon}(A)$. Hence, ξ extends to a simplicial map also between Vietoris-Rips complexes.

3.1. Homology Groups via Vietoris-Rips Complex

We use the following fundamental result from [19] to compute the homology groups of X from a filtration of Vietoris-Rips complexes on a finite sample.

Theorem 3.2 (Hausmann's Theorem [19]). Let X be a geodesic subspace with a positive convexity radius ρ . For $0 < \varepsilon < \rho$, there exists a homotopy equivalence $T : |\mathcal{R}_{\varepsilon}^{L}(X)| \longrightarrow X$.

Note that $\mathcal{R}_{\varepsilon}^{L}(X)$ is usually an infinite Vietoris-Rips complex on the entire space X. A quick corollary of this result is:

373

376

380

381

382

383

387

388

389

Corollary 3.3. Let X be a geodesic subspace with a positive convexity radius ρ . For $0 < \varepsilon' \le \varepsilon < \rho$, the inclusion $i : \mathcal{R}_{\varepsilon'}^L(X) \hookrightarrow \mathcal{R}_{\varepsilon}^L(X)$ induces isomorphisms on homology and homotopy groups.

In order to achieve our result, we use certain simplicial maps to compare $\mathcal{R}_*^L(X)$, $\mathcal{R}_*(X)$, and $\mathcal{R}_*(S)$.

Lemma 3.4 (Euclidean and Intrinsic Rips Complexes). Let X a geodesic subspace of \mathbb{R}^N with a finite distortion δ . Then for $A \subseteq X$ and any positive number α , we have the following simplicial inclusions

$$\mathcal{R}^{L}_{\alpha}(A) \hookrightarrow \mathcal{R}_{\alpha}(A) \hookrightarrow \mathcal{R}^{L}_{\delta\alpha}(A).$$

Proof. The fact that $||x-y||_2 \le d_L(x,y)$ implies the first inclusion $\mathcal{R}^L_{\alpha}(A) \hookrightarrow \mathcal{R}_{\alpha}(A)$.

Similarly, $d_L(x,y) \le \delta ||x-y||_2$ implies the second inclusion.

Theorem 3.5 (Reconstruction via Rips Complex). Let X be a geodesic subspace of \mathbb{R}^N with a positive convexity radius ρ and finite distortion δ . Let S be a finite subset of \mathbb{R}^N , and let ε be a positive number such that

$$d_H(X,S) < \frac{\varepsilon}{4} < \frac{\rho}{2\delta(3\delta+2)}.$$

Then, for any non-negative integer k we have the following isomorphism

$$H_k(X) \cong \operatorname{im}(j_* : H_k(\mathcal{R}_{\varepsilon}(S)) \longrightarrow H_k(\mathcal{R}_{\frac{1}{2}(3\delta+1)\varepsilon}(S)))$$

where j_* is induced by the simplicial inclusion $j: \mathcal{R}_{\varepsilon}(S) \longrightarrow \mathcal{R}_{\frac{1}{2}(3\delta+1)\varepsilon}(S)$.

Proof. We derive the following chain of simplicial maps:

$$\mathcal{R}^{L}_{\frac{\varepsilon}{2}}(X) \xrightarrow{\phi_{1}} \mathcal{R}_{\varepsilon}(S) \xrightarrow{\phi_{2}} \mathcal{R}^{L}_{\frac{3\varepsilon}{2}\delta}(X) \xrightarrow{\phi_{3}} \mathcal{R}_{(3\delta+1)\frac{\varepsilon}{2}}(S) \xrightarrow{\phi_{4}} \mathcal{R}^{L}_{\frac{1}{2}(3\delta+2)\delta\varepsilon}(X). \tag{4}$$

The first map ϕ_1 is the composition of the simplicial inclusion $\mathcal{R}^{\underline{L}}_{\underline{\varepsilon}}(X) \longrightarrow \mathcal{R}_{\underline{\varepsilon}}(X)$ from Lemma 3.4 and the simplicial map $\mathcal{R}_{\underline{\varepsilon}}(X) \longrightarrow \mathcal{R}_{\varepsilon}(S)$ from Lemma 3.1, thanks to the assumption $d_H(S,X) < \underline{\varepsilon}_A$.

Now, starting with $\mathcal{R}_{\varepsilon}(S)$ and composing maps from Lemma 3.1 and Lemma 3.4, respectively, we get the second simplicial map ϕ_2 . Similarly, we get the maps ϕ_3 and ϕ_4 .

From Lemma 3.1, we first note that the composition $\phi_3 \circ \phi_2$ is contiguous to the inclusion:

$$j: \mathcal{R}_{\varepsilon}(S) \longrightarrow \mathcal{R}_{(3\delta+1)\frac{\varepsilon}{\varepsilon}}(S).$$

Therefore, they induce homotopic maps on the respective underlying topological spaces. Consequently, we have $(\phi_3 \circ \phi_2)_* = j_*$. We first argue that ϕ_{2_*} is surjective and ϕ_{3_*} is injective.

By the choice of the simplicial maps in Lemma 3.4 and Lemma 3.1, we observe that $\phi_2 \circ \phi_1$ is contiguous to the inclusion

$$\mathcal{R}^{L}_{\frac{\varepsilon}{2}}(X) \longrightarrow \mathcal{R}^{L}_{\frac{3\varepsilon}{2}\delta}(X).$$

392

393

401

402

403

411

412

413

414

417

By Corollary 3.3, the inclusion induces isomorphism on homology, hence so does $\phi_2 \circ \phi_1$. In particular, $(\phi_2 \circ \phi_1)_*$ is surjective. Hence, we have ϕ_{2_*} is surjective, and ϕ_{1_*} is injective.

Also, $\phi_4 \circ \phi_3$ is contiguous to the inclusion

$$\mathcal{R}^{L}_{\frac{3\varepsilon}{2}\delta}(X) \longrightarrow \mathcal{R}^{L}_{\frac{1}{2}(3\delta+2)\delta\varepsilon}(X),$$

which induces an isomorphism on homologies. Therefore, ϕ_{3*} induces an injective homomorphism.

Since we have $j_* = \phi_{3_*} \circ \phi_{2_*}$ and ϕ_{2_*} is surjective, the image of j_* is the image of ϕ_{3_*} .

On the other hand, we know that $Im(\phi_{3_*})$ is isomorphic to $H_*\left(\mathcal{R}^L_{\frac{3_{\varepsilon}}{2}\delta}(X)\right)/Ker(\phi_{3_*})$. As we have already shown that ϕ_{3_*} is injective, its kernel is trivial. Therefore, the image of j_* is isomorphic to $\mathcal{R}^L_{\frac{3_{\varepsilon}}{2}\delta}(X)$. Since $\frac{3_{\varepsilon}}{2}\delta < \rho$, Theorem 3.2 implies that $\mathcal{R}^L_{\frac{3_{\varepsilon}}{2}\delta}(X)$ is, in fact, homotopy equivalent to X. This completes the proof.

The Vietoris-Rips reconstruction result works also for an infinite sample S. In applications, however, we are computationally constrained to use only finite samples.

3.2. Homology Groups via Čech Complex

The reconstruction of homology groups via the Vietoris-Rips filtration (see Theorem 3.5 in Section 3.1) was due to the homotopy equivalence theorem (Theorem 3.2). In this subsection, we use Čech filtration to obtain similar reconstruction results. The Nerve Lemma (Lemma 2.5) is resorted to as the Čech alternative to Theorem 3.2. Like the Vietoris-Rips case, we still use different simplicial maps to compare $\mathcal{C}_*^L(X)$, $\mathcal{C}_*(X)$, and $\mathcal{C}_*(S)$. The approach involves a (controlled) variant of the partition of unity; see Lemma 3.8.

Lemma 3.6 (Euclidean and Intrinsic Čech Complexes). Let X a geodesic subspace of \mathbb{R}^N with a finite distortion δ . Then for $A \subseteq X$ and any positive number α , we have the following simplicial inclusions

$$\mathcal{C}^{L}_{\varepsilon}(A) \longrightarrow \mathcal{C}_{\alpha}(A) \longrightarrow \mathcal{C}^{L}_{2\delta\alpha}(A).$$

Proof. From $||x-y||_2 \le d_L(x,y)$, we have the first inclusion.

On the other hand, for any $x, y \in X$ we have $d_L(x, y) \leq \delta ||x - y||_2$. Let $\sigma = \{x_0, ..., x_k\}$ be a simplex of $\mathcal{C}_{\alpha}(A)$. Then $||x_i - x_j||_2 < 2\alpha$, consequently $d_L(x_i, x_j) < 2\delta\alpha$ for all $1 \leq i, j \leq k$. This implies

$$\{x_0, x_1, \dots, x_k\} \subset \bigcap_{i=0}^k \mathbb{B}^L(x_i, 2\delta\alpha),$$

where $\mathbb{B}^L(x_i, r)$ denotes the ball of radius r centered at x_i in the metric space (X, d_L) .

Therefore $\sigma \in \mathcal{C}^L_{2\delta\alpha}(A)$, and this verifies the second inclusion.

We begin with a lemma that is analogous to Corollary 3.3 in the Čech regime:

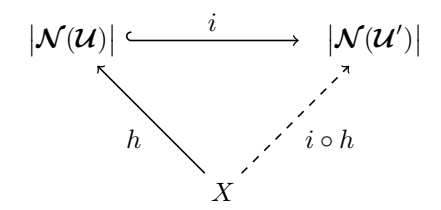
433

Lemma 3.7 (Inclusion of Covers). Let $\mathcal{U} = \{U_i\}_{i \in \Lambda}$ and $\mathcal{U}' = \{U_i'\}_{i \in \Lambda}$ be locally-finite, good open covers of a para-compact topological space X such that $U_i \subseteq U'_i$ for each i. Then, 419 the inclusion 420

$$i: \mathcal{N}(\mathcal{U}) \hookrightarrow \mathcal{N}(\mathcal{U}')$$

induces isomorphisms on the homology and homotopy groups of the respective geometric 422 complexes. 423

Proof. Consider the following commutative diagram:



where the map $h = \sum \varphi_i u_i$ is obtained from an arbitrary partition of unity $\{\varphi_i\}$ for \mathcal{U} . By the Nerve Lemma (Lemma 2.5), h is a homotopy equivalence ([23]). Since $U_i \subseteq U_i'$, $\{\varphi_i\}$ 425 is a partition of unity for \mathcal{U}' . So, $i \circ h$ is also a homotopy equivalence. Since the maps h is a homotopy equivalence, we conclude that i induces an isomorphism on homology and 427 homotopy groups.

We now state the following extension of the partition of unity. Follow [30] for a proof. 429

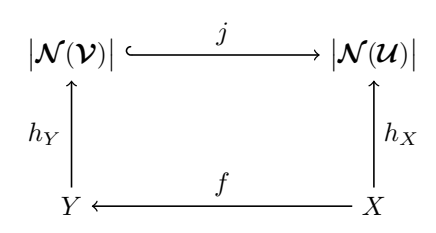
Lemma 3.8 (Controlled Partition of Unity). Let $\{U_i\}$ and $\{V_i\}$ be open covers of a paracompact, Hausdorff space X such that $\overline{V_i} \subseteq U_i$ for each i. Then, there exists a partition 431 of unity $\{\varphi_i\}$ subordinate to $\{U_i\}$ such that $V_i \subseteq supp \ \varphi_i \subseteq U_i$ for all i. 432

We now use the controlled partition of unity to prove the following important lemma.

Lemma 3.9 (Commuting Diagram). Let X, Y be paracompact, Hausdorff spaces with a 434 continuous map $f: X \to Y$. Let $\mathcal{U} = \{U_i\}$ and $\mathcal{V} = \{V_i\}$ be good, locally finite, open covers 435 of X and Y respectively, such that 436

- (1) $\bigcap_i V_i \neq \emptyset$ implies $\bigcap_i U_i \neq \emptyset$, i.e., we have the simplicial inclusion $j: \mathcal{N}(\mathcal{V}) \to \mathcal{N}(\mathcal{U})$ that sends the vertex corresponding to V_i to the vertex corresponding to U_i , 438
- (2) $\overline{f^{-1}(V_i)} \subseteq U_i$ for all i.

Then, the following diagram commutes, up to homotopy:



where h_X , h_Y are homotopy equivalences from (3).

Proof. We make use of the controlled partition of unity lemma to prove our result. Let us choose a partition of unity $\{\phi_i\}$ subordinate to $\{V_i\}$. One can choose h_Y so that for each $y \in Y$,

$$h_Y(y) = \sum_i \phi_i(y) v_i,$$

where v_i is the vertex of $\mathcal{N}(\mathcal{V})$ corresponding to V_i .

Since $\{f^{-1}(V_i)\}$ is an open cover of X with $\overline{f^{-1}(V_i)} \subseteq U_i$ for each i, by Lemma 3.8 we can choose a partition of unity $\{\psi_i\}$ subordinate to $\{U_i\}$ such that for each i

$$f^{-1}(V_i) \subseteq \operatorname{supp} \psi_i$$
.

Also, choose h_x such that for each $x \in X$

444

448

450

454

460

468

$$h_X(x) = \sum_i \psi_i(x) u_i,$$

where u_i is the vertex of $\mathcal{N}(\mathcal{U})$ corresponding to U_i .

To see that the diagram commutes, up to homotopy, it suffices to show that $(j \circ h_Y \circ f)$ is homotopic to h_X . We start with a point $x_0 \in X$

$$(j \circ h_Y \circ f)(x_0) = j(\sum_i \phi_i(f(x_0))v_i) = \sum_i \phi_i(f(x_0))j(v_i) = \sum_i \phi_i(f(x_0))u_i.$$

On the other hand, $h_X(x_0) = \sum_i \psi_i(x_0)u_i$. Now if $\phi_i(f(x_0))$ is non-zero for some i, then $f(x_0) \in V_i$, and consequently $x_0 \in f^{-1}(V_i) \subseteq U_i$. From our choice of the support of ψ_i and $\psi_i(x_0)$ has to be non-zero. This shows that both $(j \circ h_Y \circ f)(x_0)$ and $h_X(x_0)$ lie in an (open) simplex of $\mathcal{N}(\mathcal{V})$. Due to convexity of simplices, the following (straight-line) homotopy is well-defined:

$$F(x,t) = \sum_{i} [t\psi_{i}(x) + (1-t)\phi_{i}(x)] u_{i}.$$

This shows that $(j \circ h_Y \circ f)$ is homotopic to h_X .

Now we are in a position to prove our reconstruction result for Čech complexes.

Theorem 3.10 (Reconstruction via Čech complex). Let X be a geodesic subspace of \mathbb{R}^N with a positive convexity radius ρ and finite distortion δ . Let S be a finite subset of \mathbb{R}^N , and let ε be a positive number such that

$$d_H(X,S) < \varepsilon < \frac{\rho}{2\delta(4\delta+1)}.$$

Then, any non-negative integer k we have the following isomorphism

$$H_k(X) \cong \operatorname{im}(j_* : H_k(\mathcal{C}_{\varepsilon}(S)) \longrightarrow H_k(\mathcal{C}_{(4\delta+1)\varepsilon}(S)))$$
 (5)

where j_* is induced by the simplicial inclusion $j: \mathcal{C}_{\varepsilon}(S) \longrightarrow \mathcal{C}_{(4\delta+1)\varepsilon}(S)$.

475

476

477

478

479

480

481

483

485

486

487

488

489

490

491

492

493

495

496

497

498

499

500

Proof. We first note from $d_H(X,S) < \varepsilon$ and Lemma 3.1 that there is a map $\xi: S \to X$ such that for each $s \in S$, 471

$$\|s - \xi(s)\|_2 < \varepsilon. \tag{6}$$

Let $X' = \xi(S)$. Then, (6) implies $d_H(S, X') < \varepsilon$, hence $d_H(X, X') < 2\varepsilon$ by the triangle 473 inequality. 474

We now derive the following chain of simplicial maps:

$$\mathcal{C}_{\varepsilon}(S) \xrightarrow{\phi_1} \mathcal{C}_{4\varepsilon\delta}^L(X') \xrightarrow{\phi_2} \mathcal{C}_{(4\delta+1)\varepsilon}(S) \xrightarrow{\phi_3} \mathcal{C}_{2\delta(4\delta+1)\varepsilon}^L(X').$$

The first map ϕ_1 is the composition of the simplicial map $\mathcal{C}_{\varepsilon}(S) \longrightarrow \mathcal{C}_{2\varepsilon}(X')$ from Lemma 3.1 (due to $d_H(S, X') < \varepsilon$) and the simplicial inclusion $\mathcal{C}_{2\varepsilon}(X') \longleftrightarrow \mathcal{C}_{4\delta\varepsilon}^L(X')$ from Lemma 3.6.

Similarly, starting with $\mathcal{C}_{4\delta\varepsilon}^L(X')$ and composing maps from Lemma 3.6 and Lemma 3.1, respectively, we get the second simplicial map ϕ_2 . The other map ϕ_3 is also obtained repeating the exact same argument for a different scale as for ϕ_1 .

We first observe that the choice of simplicial maps in Lemma 3.6 and Lemma 3.1 makes $\phi_2 \circ \phi_1$ contiguous to the given natural inclusion j of $\mathcal{C}_{\varepsilon}(S)$ into $\mathcal{C}_{2\delta(4\delta+1)\varepsilon}(S)$. We now consider the following diagram:

$$\begin{aligned} |\mathcal{C}_{\varepsilon}(S)| & \xrightarrow{\phi_{1}} & |\mathcal{C}_{4\delta\varepsilon}^{L}(X')| & \xrightarrow{\phi_{2}} & |\mathcal{C}_{(4\delta+1)\varepsilon}(S)| & \xrightarrow{\phi_{3}} & |\mathcal{C}_{2\delta(4\delta+1)\varepsilon}^{L}(X')| \\ h_{1} & & h_{2} & & & h_{3} \\ S^{\varepsilon} & & & i & & X & & Id & & X \end{aligned}$$

To show that the diagram commutes up to homotopy, we first explain the horizontal maps in the bottom row of (7). Since $d_H(X,S) < \varepsilon$, we get the first inclusion $X \subseteq S^{\varepsilon}$. The three vertical maps are homotopy equivalences that come from the Nerve Lemma (Lemma 2.5) for various good open covers as constructed in Lemma 3.9. The first vertical map h_1 is obtained for the open cover $\mathcal{U}_1 = \{\mathbb{B}(x,\varepsilon)\}_{x\in S}$ of S^{ε} by Euclidean balls. The other two vertical maps, h_2 and h_3 , are corresponding to the (intrinsic) covers \mathcal{U}_2 and \mathcal{U}_3 of (X, d_L) by the intrinsic balls of radii $2\delta\varepsilon$ and $4\delta(2\delta+1)\varepsilon$, respectively. The assumption $4\delta(2\delta+1)\varepsilon < \rho$ implies that they are indeed good (intrinsic) covers of X. Therefore, by Lemma 2.7 we get the homotopy equivalences h_2 and h_3 .

Apply Lemma 3.9 to each of the rectangles in (7) to show that the diagram is homotopy commutative, and therefore it commutes on the homology level. The commutativity then implies that ϕ_1 induces a surjective homomorphism and ϕ_2 induces an injective homomorphism on the homology groups. As a consequence, $\operatorname{Im}(\phi_{2*} \circ \phi_{1*}) = \operatorname{Im}(\phi_{2*}) = H_k(X)$ on the k-th homology group. Also, we note that $\phi_2 \circ \phi_1$ is homotopic to the given simplicial inclusion j.

To see that the first rectangle commutes, we consider the covers \mathcal{U}_1 and \mathcal{U}_2 of S^{ε} and (X, d_L) . Note that for any $x \in S$, the choice of $\xi(x)$ implies that $i^{-1}(\mathbb{B}(x, \varepsilon)) = \mathbb{B}(x, \varepsilon) \cap$ $\mathbb{B}^{L}(\xi(x), 2\delta\varepsilon)$. Consequently, $\overline{\mathbb{B}(x,\varepsilon)\cap X}\subseteq \mathbb{B}^{L}(\xi(x), 4\delta\varepsilon)$. A similar argument also applies to other rectangle. Therefore by Lemma 3.9, the diagram (7) commutes.

Remark 3.11. We remark that Theorem 3.5 and Theorem 3.10 of this section can be formulated in terms of any natural functor from the category of topological spaces (with continuous maps as morphisms) to the category of groups (with group homomorphisms). In particular, the results extend immediately to homology groups $H_*(\cdot; G)$ with coefficients in any abelian group G, or homotopy groups $\pi_*(\cdot)$.

4. Geometric Reconstruction

In the previous section, we used filtrations of both the Čech and the Vietoris-Rips complexes to compute the homology and homotopy groups of our hidden geodesic subspace X from a noisy sample S around it. The results, however, do not provide us with a topological space that faithfully carries the topology of X. To remedy this, we consider the problem of geometric reconstruction of geodesic subspaces.

In Section 4.1, we introduce a new metric d_{ε} on S. As our first step towards capturing the homotopy type, we show in Theorem 4.3 that the Vietoris-Rips complex of (S, d_{ε}) and X have isomorphic fundamental groups. Finally in Section 4.2, we further use this complex for the geometric reconstruction of embedded graphs.

4.1. Recovery of the Fundamental Group

For any fixed $\varepsilon > 0$, we first consider the Euclidean Vietoris-Rips complex $\mathcal{R}_{\varepsilon}(S)$ on the sample S. Regardless of how dense the sample S is, $\mathcal{R}_{\varepsilon}(S)$ is not guaranteed to be homotopy equivalent to X in general; as shown in Figure 5. This is not surprising, because the Euclidean metric on S, used to compute the complex, can be very different from the length metric d_L on X. Our goal is to approximate d_L by the shortest path metric, denoted d_{ε} , on the one-skeleton of $\mathcal{R}_{\varepsilon}(S)$. Let us denote the one-skeleton of $\mathcal{R}_{\varepsilon}(S)$ by G_{ε} . Since $\mathcal{R}_{\varepsilon}(S)$ is an abstract simplicial complex, G_{ε} inherits the structure of an abstract graph. However, we turn its geometric complex $|G_{\varepsilon}|$ into a metric graph by defining the metric d_{ε} on it in the following way: the metric, when restricted to an edge (s,t), is isometric to a real interval of length $||s-t||_2$.

We show in Lemma 4.1 that d_{ε} nicely approximates the metric d_L , which the Euclidean sample is oblivious to. For any positive scale α , we denote the Vietoris-Rips complex of S in the d_{ε} metric by $\mathcal{R}_{\alpha}^{\varepsilon}(S)$. The metric d_{ε} can be computed in $O(k^3)$ -time from a sample (S, d_2) of size k. In the following lemma, we compare the metric d_{ε} with the standard Euclidean metric d_2 and the length metric d_L .

Lemma 4.1 (Minimal Covering of Paths). Let X be a geodesic subspace of \mathbb{R}^N . Let S be a subset of \mathbb{R}^N and $\varepsilon > 0$ such that $d_H(X,S) < \frac{\varepsilon}{3}$. For any path γ joining any two points $x, y \in X$, we can find a sequence $\{a_i\}_{i=0}^k \subseteq S$ with $||a_{i+1} - a_i||_2 < \varepsilon$ such that

$$\sum_{i=0}^{k-1} \|a_{i+1} - a_i\|_2 < 3l(\gamma).$$

Moreover, a_0 and a_k can be chosen to be any points with $||x - a_0||_2 < \frac{\varepsilon}{3}$ and $||y - a_K||_2 < \frac{\varepsilon}{3}$.

Proof. Since $d_H(X,S) < \frac{\varepsilon}{3}$, there exists $a_0 \in S$ such that $||x - a_0||_2 < \frac{\varepsilon}{3}$. We now iteratively define the sequence $\{a_i\}\subseteq S$, along with a sequence $\{t_i\}_0^k\subset [0,1]$ that defines a partition of [0, 1]. We set $t_0 = 0$. Assuming both a_i and t_i are defined, we define $t_{i+1} \in [0, 1]$ in the following way: if $\gamma([t_i,1]) \cap \partial \mathbb{B}\left(a_i,\frac{2\varepsilon}{3}\right) \neq \emptyset$, we set

$$t_{i+1} = \min\{t \in [t_i, 1] \mid \gamma(t) \in \partial \mathbb{B}\left(a_i, \frac{2\varepsilon}{3}\right)\}.$$

Otherwise if $\gamma([t_i, 1]) \cap \partial \mathbb{B}\left(a_i, \frac{2\varepsilon}{3}\right) = \emptyset$, set $t_{i+1} = 1$. Since $d_H(S, X) < \frac{\varepsilon}{3}$, we set $a_{i+1} \in S$ to be a point in S such that $\|\gamma(t_{i+1}) - a_{i+1}\|_2 < \frac{\varepsilon}{3}$. This procedure forces t_{i+1} to be strictly 542 greater than t_i , hence $\{t_i\}$ defines a partition of [0,1]. Therefore,

$$l(\gamma) = \sum_{i=0}^{k} l(\gamma|_{[t_i, t_{i+1}]}) \ge \sum_{i=0}^{k} \|\gamma(t_i) - \gamma(t_{i+1})\|_2 \ge \sum_{i=0}^{k} \frac{\varepsilon}{3} \ge \frac{1}{3} \sum_{i=0}^{k} \|a_{i+1} - a_i\|_2.$$

We also note that

540

544

546

551

553

557

560

561

562

563

$$0 < \|a_{i+1} - a_i\|_2 \le \|a_{i+1} - \gamma(t_{i+1})\|_2 + \|\gamma(t_{i+1}) - a_i\|_2 < \frac{\varepsilon}{3} + \frac{2\varepsilon}{3} = \varepsilon.$$

Analogous to Lemma 3.1, we get the following useful simplicial maps.

Lemma 4.2 (Vietoris-Rips Inclusion by d_{ε}). Let X a geodesic subspace $X \subseteq \mathbb{R}^N$. Let $\subseteq \mathbb{R}^N$ and $\varepsilon > 0$ be such that $d_H(X,S) < \frac{\varepsilon}{3}$. For any $\alpha > 0$,

(1) there exists a natural simplicial inclusion

$$\mathcal{R}^{\varepsilon}_{\alpha}(S) \longrightarrow \mathcal{R}_{\alpha}(S).$$

(2) there exists a simplicial map 552

$$\xi: \mathcal{R}^L_{\alpha}(X) \longrightarrow \mathcal{R}^{\varepsilon}_{3\alpha}(S)$$

induced by the vertex map ξ that sends a vertex $x \in X$ to $s \in S$ such that $||x - s||_2 < \frac{\varepsilon}{3}$.

555

- (1) Follows immediately from the definition of the metric d_{ε} .
- (2) As observed before in Lemma 3.1, the assumption $d_H(X,S) < \frac{\varepsilon}{3}$ ensures that there is a vertex map $\xi: X \to S$ such that for each $x \in X$ we have $||x - \xi(x)||_2 < \frac{\varepsilon}{3}$.

We show that the map extends to a simplicial map. Let $\sigma = \{x_0, x_1, \dots, x_k\}$ be a k-simplex of $\mathcal{R}^L_{\alpha}(X)$. Then, $d_L(x_i, x_j) \leq \alpha \ \forall i, j$. Now by Lemma 4.1, there exists a path joining $\xi(x_i)$ and $\xi(x_i)$ in G_{ε} , moreover $d_{\varepsilon}(\xi(x_i), \xi(x_i)) < 3\alpha$. So, $\xi(\sigma)$ is a simplex of $\mathcal{R}_{3\alpha}^{\varepsilon}(S)$. Hence, the vertex map extends to a simplicial map.

We now show that the fundamental group of the Vietoris-Rips complex on S under the metric d_{ε} is isomorphic to that of X. We tolerate the sloppiness from ignoring the basepoint.

567

568

572

573

577

578

579

580

581

582

583

587

Theorem 4.3 (Fundamental Group). Let X be a connected geodesic subspace of \mathbb{R}^N with a positive convexity radius ρ and a finite distortion δ . Let $S \subseteq \mathbb{R}^N$ and $\varepsilon > 0$ be such that

$$d_H(X,S) < \frac{\varepsilon}{3} < \frac{\rho}{\delta(15\delta + 2)}.$$

Then, the fundamental groups of $\mathcal{R}^{\varepsilon}_{5\varepsilon\delta}(S)$ and X are isomorphic.

Proof. We derive the following chain of simplicial maps:

$$\mathcal{R}_{\varepsilon}(S) \xrightarrow{\phi_{1}} \mathcal{R}_{\frac{5\varepsilon\delta}{2}}^{L}(X) \xrightarrow{\phi_{2}} \mathcal{R}_{5\delta\varepsilon}^{\varepsilon}(S) \xrightarrow{\phi_{3}} \mathcal{R}_{5\delta\varepsilon}(S) \xrightarrow{\phi_{4}} \mathcal{R}_{\delta(15\delta+2)\varepsilon/3}^{L}(X).$$

The map ϕ_1 is the composition of the simplicial map $\mathcal{R}_{\varepsilon}(S) \longrightarrow \mathcal{R}_{\frac{5\varepsilon}{3}}(X)$ from Lemma 3.1 and the simplicial inclusion $\mathcal{R}_{\frac{5\varepsilon}{3}}(X) \hookrightarrow \mathcal{R}_{\frac{5\varepsilon}{3}}^L(S)$ from Lemma 3.4, thanks to the assumption $d_H(S,X) < \frac{\varepsilon}{3}$. By a similar composition but at different scales, we get ϕ_4 . We also obtain ϕ_2 from Lemma 4.2 and ϕ_3 from Lemma 4.2.

We argue that ϕ_2 induces the desired isomorphism on the fundamental groups. By Theorem 3.5 and since $\varepsilon < \frac{\rho}{\delta(15\delta+2)}$, the simplicial map $\phi_4 \circ \phi_3 \circ \phi_2$ induces an isomorphism on all homotopy groups. Therefore, ϕ_2 induces an injective homomorphism on the homotopy groups, particularly the fundamental group of X.

We now show that the induced homomorphism is also surjective on the fundamental groups by showing that $\phi_2 \circ \phi_1$ induces a surjection. As observed Theorem 3.5, it suffices to show the surjection for the natural inclusion $i: \mathcal{R}_{\varepsilon}(S) \longrightarrow \mathcal{R}^{\varepsilon}_{5\delta\varepsilon}(S)$, because i is contiguous to $\phi_2 \circ \phi_1$.

We start with a loop η in $\mathcal{R}^{\varepsilon}_{5\delta\varepsilon}(S)$. We can assume that η is made up of edges (one-simplices) of $\mathcal{R}^{\varepsilon}_{5\delta\varepsilon}$. Let us consider an edge $\sigma = \{a,b\}$ in η , then we have $d_{\varepsilon}(a,b) \leq 5\delta\varepsilon$. By the definition of d_{ε} , there must be a sequence of points $a = x_0, x_1, \dots, x_k = b$ such that for each i, the segment $[x_i, x_{i+1}]$ is an edge of $\mathcal{R}_{\varepsilon}(S)$. Moreover, we observe for later that the diameter of the whole set $\{x_0, \dots, x_k\}$ in the d_{ε} metric is not greater than $5\varepsilon\delta$.

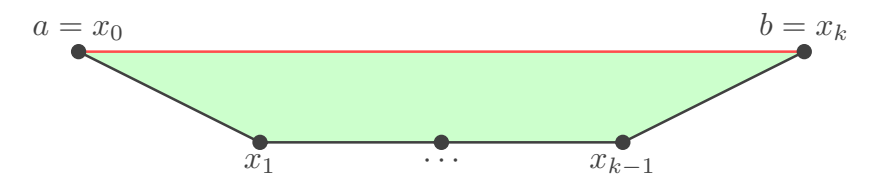


Fig. 4: The red one-simplex [a,b] of $\mathcal{R}^{\varepsilon}_{5\delta\varepsilon}(S)$ is shown to be pushed off to a path $a=x_0,x_1,\cdots,x_k=b$ in $\mathcal{R}_{\varepsilon}(S)$. All the nodes form a simplex (shown in green) in $\mathcal{R}^{\varepsilon}_{5\delta\varepsilon}(S)$.

Now, we define a loop η' in $\mathcal{R}_{\varepsilon}(S)$ by replacing each constituent edge [a,b] of η by the path joining the points in the sequence $a=x_0,x_1,\cdots,x_k=b$ consecutively, as shown in Figure 4. We note that η' is indeed a loop in $\mathcal{R}_{\varepsilon}(S)$. We now show that $(\phi_2 \circ \phi_1)(\eta')$ is homotopic to the loop η in $\mathcal{R}_{5\delta\varepsilon}^{\varepsilon}(S)$. As observed before, $\{a=x_0,\cdots,x_k=b\}$ is a simplex

601

602

603

604

605

609

610

611

613

614

615

616

617

618

619

of $\mathcal{R}_{5\delta\varepsilon}^{\varepsilon}(S)$. We can then use a (piece-wise) straight line homotopy that maps each edge [a,b] of η to the segment $[a=x_0,x_1]\cup\cdots\cup[x_{k-1},x_k=b]$ of η' . Hence, $[\eta']$ is, in fact, a preimage of $[\eta]$. This shows, in turn, that ϕ_2 induces a surjective homomorphism on π_1 . This completes the proof.

4.2. Reconstruction of Embedded Graphs

We finally turn our attention to the geometric reconstruction of embedded graphs. We start with the formal definition of an embedded graph.

Definition 4.4 (Embedded Metric Graph). An embedded metric graph G is a subset of \mathbb{R}^N that is homeomorphic to a one-dimensional simplicial complex, where the induced length metric d_L is the shortest path distance on G. For simplicity of exposition, we call such G embedded graphs.

We note that if G has finitely many vertices and b is the length of its shortest simple cycle, then the convexity radius ρ is $\frac{b}{4}$. In this paper, we always assume that G has finitely many vertices. We now consider the *shadow* of the Vietoris-Rips complex $\mathcal{R}^{\varepsilon}_{\bullet}(S)$, which is defined in Section 4.1.

Definition 4.5 (Shadow of a Complex). Let A be a subset of \mathbb{R}^N , and let \mathcal{K} be an abstract simplicial complex whose vertex set is A. For each simplex $\sigma = \{x_1, x_2, \dots, x_k\}$ in \mathcal{K} , we define its shadow, denoted $\mathbf{Sh}(\sigma)$, as the convex-hull of the Euclidean point set $\{x_1, x_2, \dots, x_k\}$. The shadow of \mathcal{K} in \mathbb{R}^N , denoted by $\mathbf{Sh}(\mathcal{K})$, is the union of the shadows of all its simplices, i.e., $\mathbf{Sh}(\mathcal{K}) := \bigcup_{\sigma \in \mathcal{K}} \mathbf{Sh}(\sigma)$.

We, therefore, have the following natural projection map $p: |\mathcal{K}| \to \mathbf{Sh}(\mathcal{K})$. In general, $\mathbf{Sh}(\mathcal{K})$ may not have the same homotopy type as $|\mathcal{K}|$. However, as proved in [31], the fundamental group of the Vietoris-Rips complex of a planar point set is isomorphic to the fundamental group of its shadow. In [16], the authors further the understanding of shadows of Euclidean Rips complexes. In the case of planar subsets and $\mathcal{K} = \mathcal{R}^{\varepsilon}_{\bullet}(S)$, we prove a similar result now.

Lemma 4.6 (Shadow). Let X be a connected planar subspace with a positive convexity radius ρ and a finite distortion δ . Given $S \subseteq \mathbb{R}^2$ finite and $\varepsilon > 0$ such that

$$d_H(X,S) < \frac{\varepsilon}{3} < \frac{\rho}{\delta(15\delta + 2)}.$$

Then, the shadow projection $p: \left| \mathcal{R}_{5\varepsilon\delta}^{\varepsilon}(S) \right| \longrightarrow \mathbf{Sh}(\mathcal{R}_{5\varepsilon\delta}^{\varepsilon}(S))$ induces isomorphism on the fundamental groups.

Proof. From Theorem 4.3, we have the following chain of simplicial maps:

$$\mathcal{R}_{\varepsilon}(S) \xrightarrow{\phi_1} \mathcal{R}^L_{5\varepsilon\delta/3}(X) \xrightarrow{\phi_2} \mathcal{R}^{\varepsilon}_{5\delta\varepsilon}(S) \xrightarrow{\phi_3} \mathcal{R}_{5\delta\varepsilon}(S) \xrightarrow{\phi_4} \mathcal{R}^L_{\delta(15\delta+2)\varepsilon/3}(X).$$

We have shown that ϕ_2 induces an isomorphism on π_1 . As we have also noted that $(\phi_4 \circ \phi_3 \circ \phi_2)$ induces an isomorphism on all homotopy groups. So, we conclude first that ϕ_3 induces an injective homomorphism on π_1 .

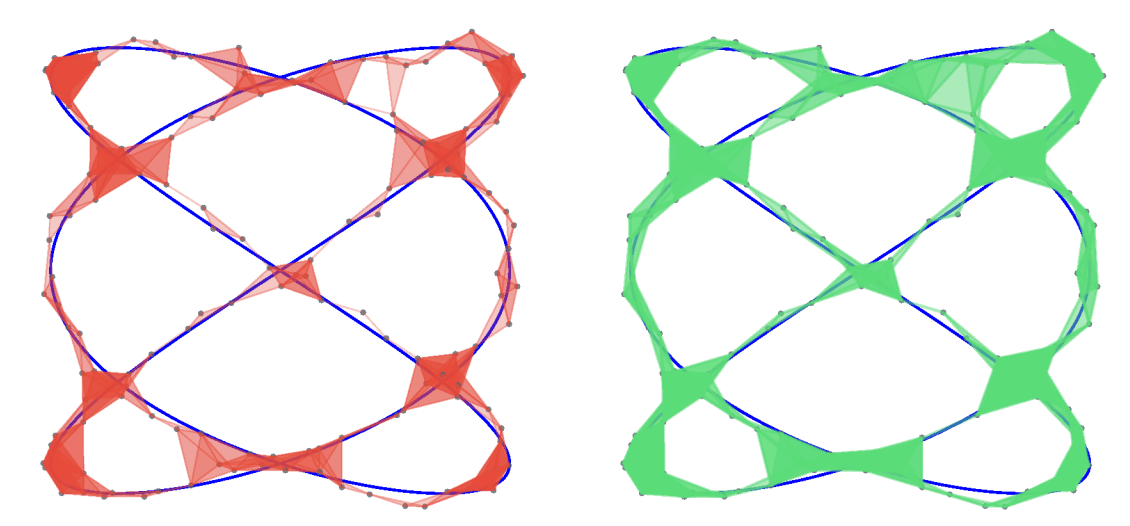


Fig. 5: We implement Algorithm 1 on a Lissajous G with $\beta_1(G) = 8$. On the left, the Euclidean Vietoris-Rips complex $\mathcal{R}_{\varepsilon}(S)$ (in red) on an ε -dense sample S of 150 points fails to capture the homotopy type, as its $\beta_1 = 9$. On the right, the shadow \widetilde{G} (green) of $\mathcal{R}_{5\delta\varepsilon}^{\varepsilon}(S)$ is shown to correctly reconstruct G. The pictures were generated using the shape reconstruction library available on www.smajhi.com/shape-reconstruction.

Now, we consider the following commutative diagram:

625

627

628

629

631

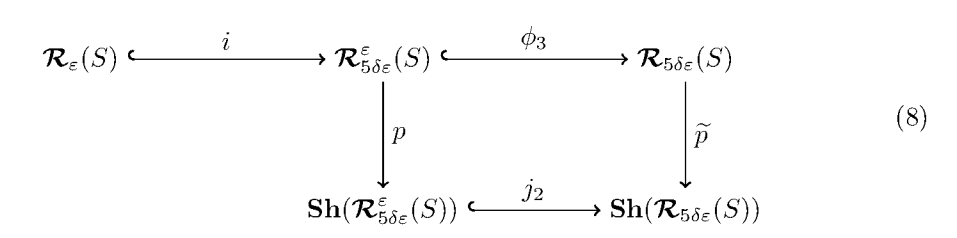
632

633

634

635

636



where i is contiguous to the composition $(\phi_2 \circ \phi_1)$, and p, \tilde{p} are the natural (shadow) projections.

We show that the induced map p_* is an isomorphism on the fundamental groups. From the commutativity of the diagram (8), we note that p_* is an injection on π_1 , since ϕ_{3_*} is injective and \widetilde{p}_* is also injective on π_1 by [31]. For surjectivity, we follow the same lifting argument presented in [31].

As a consequence of Lemma 4.6, we finally present our main geometric reconstruction result.

Theorem 4.7 (Geometric Reconstruction of Planar Subspaces). Let X be a connected geodesic subspace of \mathbb{R}^2 with a positive convexity radius ρ and a finite distortion δ , which has the homotopy type of a finite simplicial complex. Let $S \subseteq \mathbb{R}^2$ be finite, and $\varepsilon > 0$

be such that

639

642

648

649

650

651

652

654

658

661

666

668

$$d_H(X,S) < \frac{\varepsilon}{3} < \frac{\rho}{\delta(15\delta + 2)}.$$
 (9)

Then, the shadow complex $\widetilde{X} = \mathbf{Sh}(\mathcal{R}^{\varepsilon}_{5\varepsilon\delta}(S))$ of $\mathcal{R}^{\varepsilon}_{5\varepsilon\delta}(S)$ has the homotopy type of X.

Moreover,

$$d_H(X, \widetilde{X}) < \left(5\delta + \frac{1}{3}\right)\varepsilon.$$
 (10)

Proof. By Lemma 4.6, the shadow $\widetilde{X} = \mathbf{Sh}(\mathcal{R}_{5\varepsilon\delta}^{\varepsilon}(S))$ and X have isomorphic fundamental groups, via the map p of diagram (8). Note that, by assumption, both $\mathbf{Sh}(\mathcal{R}_{5\varepsilon\delta}^{\varepsilon}(S))$ and X have a homotopy type of a finite wedge of circles and therefore trivial higher homotopy groups. By the Whitehead's theorem [32], applied to the map p, we conclude that p is a homotopy equivalence.

For statement (10), we note that for any finite vertex set $\sigma \subseteq S$ with $\operatorname{diam}(\sigma) < 5\delta\varepsilon$ we have $\sigma \subseteq \operatorname{Sh}(\sigma)$ and $d_H(\sigma, \operatorname{Sh}(\sigma)) \leq \operatorname{diam}(\sigma)$. As a consequence, $d_H(\widetilde{X}, S) \leq 5\delta\varepsilon$. By the triangle inequality, we conclude the result.

Corollary 4.8 (Geometric Reconstruction of Embedded Graphs). Let G be a finite, connected embedded graph in \mathbb{R}^2 . Let b be the length of the shortest simple cycle of G, and let δ be its distortion. Let $S \subseteq \mathbb{R}^2$ be finite and $\varepsilon > 0$ be such that

$$d_H(G,S) < \frac{\varepsilon}{3} < \frac{b}{4\delta(15\delta + 2)}.$$

Then, the shadow of $\widetilde{G} = \mathbf{Sh}(\mathcal{R}_{5\varepsilon\delta}^{\varepsilon}(S))$ has the same homotopy type as G and $\widetilde{(10)}$ holds for X = G and $\widetilde{X} = \widetilde{G}$.

Proof. It suffices to note that the convexity radius of G is $\frac{b}{4}$ and apply Theorem 4.7.

Based on Corollary 4.8, we devise Algorithm 1 for the geometric reconstruction of (planar) embedded graphs. For a demonstration, see Figure 5.

5. Discussion

In this paper, we successfully reconstruct homology/homotopy groups of general geodesic spaces. We also reconstruct the geometry of embedded graphs. Currently, the output of such geometric reconstruction is a thick region around the hidden graph; see Figure 5. One can consider a post-processing step to prune the output shadow \tilde{G} in order to output an embedded graph that is isomorphic to the hidden graph G. A natural extension of our work is to consider the geometric reconstruction of higher-dimensional simplicial complexes. Unlike the graphs, such a space may have non-trivial higher homotopy groups. The reconstruction result remains, therefore, an object of future work.

Algorithm 1 Graph Reconstruction Algorithm

```
Require: Finite sample S \subseteq \mathbb{R}^2, \varepsilon > 0, \delta, and b
Ensure: d_H(\widetilde{G},S) < \frac{\varepsilon}{3} < \frac{b}{4\delta(15\delta+2)}

1: Initialize \widetilde{G} \leftarrow \emptyset

2: Compute the one-skeleton of \mathcal{R}_{\varepsilon}(S)

3: Compute (S,d_{\varepsilon})

4: for all \{a,b,c\} \in S do

5: if d_{\varepsilon}(a,b) \leq 5\delta\varepsilon and d_{\varepsilon}(b,c) \leq 5\delta\varepsilon and d_{\varepsilon}(c,a) \leq 5\delta\varepsilon then

6: \widetilde{G} \leftarrow \widetilde{G} \cup \text{CONVEX-HULL}(\{a,b,c\})

7: end if

8: end for

9: return \widetilde{G}
```

On the other hand, we also note that both approaches are not performing well when we deform X, e.g., by "pinching" a pair of points in X, i.e., deforming X to bring these points ϵ -close in the extrinsic Euclidean distance but with bounded intrinsic distance. Creating such an ϵ -pinch generally results in a small wfs as well as large distortion of the resulting submanifold.

Based on these considerations, we conjecture that there should be a stability result within an appropriate class of geodesics subspaces of \mathbb{R}^N , saying that a fixed sample S satisfying assumptions of Theorem 3.5 and Theorem 3.10, statements (3.5) and (5) should be valid not only for a given X but also for any ϵ -close perturbation within the class. We will address this claim in the forthcoming work.

Acknowledgements

BTF was supported by grants CCF-1618605, DMS 1854336, and CCF-2046730 from the National Science Foundation. SM and CW were supported by grant CCF-1618469 from the National Science Foundation.

References

670

673

674

675

676

677

678

679

684

685

690

691

692

693

694

695

696

697

- 1. N. Amenta, M. Bern and D. Eppstein, The crust and the β -skeleton: Combinatorial curve reconstruction, *Graphical models and image processing* **60** (1998) 125.
- T. K. Dey, Curve and Surface Reconstruction: Algorithms with Mathematical Analysis (Cambridge Monographs on Applied and Computational Mathematics) (Cambridge University Press, New York, NY, USA, 2006).
 - 3. P. Niyogi, S. Smale and S. Weinberger, Finding the homology of submanifolds with high confidence from random samples, *Discrete And Computational Geometry* **39. 1-3** (2008) 419.
 - F. Chazal and A. Lieutier, Stability and computation of topological invariants of solids in ℝⁿ, Discrete & Computational Geometry 37 (2007) 601.
 - 5. F. Chazal and S. Y. Oudot, Towards persistence-based reconstruction in Euclidean spaces, in *Proc. 24th ACM Sympos. Comput. Geom.* (2008), pp. 232–241.
 - 6. F. Chazal, D. Cohen-Steiner and A. Lieutier, A sampling theory for compact sets in Euclidean space, *Discrete & Computational Geometry* **41** (2009) 461.

- 7. J. Latschev, Vietoris-Rips complexes of metric spaces near a closed Riemannian manifold, Archiv der Mathematik 77 (2001) 522.
- 8. F. Chazal, R. Huang and J. Sun, Gromov-Hausdorff approximation of filamentary structures using Reeb-type graphs, *Discrete & Computational Geometry* **53** (2015) 621.
- V. De Silva and G. Carlsson, Topological estimation using witness complexes, in *Proceedings of the First Eurographics Conference on Point-Based Graphics* (Eurographics Association, Airela-Ville, Switzerland, Switzerland, 2004), SPBG'04, pp. 157–166.
- D. Attali, A. Lieutier and D. Salinas, Vietoris-Rips complexes also provide topologically correct
 reconstructions of sampled shapes, *Computational Geometry* 46 (2013) 448, 27th Annual
 Symposium on Computational Geometry (SoCG 2011).
- H. Adams and J. Mirth, Metric thickenings of Euclidean submanifolds, Topology and its Applications 254 (2019) 69.
- 12. J. Kim, J. Shin, F. Chazal, A. Rinaldo and L. Wasserman, Homotopy reconstruction via the
 Čech complex and the Vietoris-Rips complex, in 36th International Symposium on Computational Geometry (SoCG 2020) (Schloss Dagstuhl-Leibniz-Zentrum für Informatik, 2020).
- 13. M. Aanjaneya, F. Chazal, D. Chen, M. Glisse, L. Guibas and D. Morozov, Metric graph reconstruction from noisy data, *International Journal of Computational Geometry & Applications* 22 (2012) 305.
- 14. F. Lecci, A. Rinaldo and L. A. Wasserman, Statistical analysis of metric graph reconstruction.,
 Journal of Machine Learning Research 15 (2014) 3425.
- J. Kim, J. Shin, F. Chazal, A. Rinaldo and L. Wasserman, Homotopy reconstruction via the
 cech complex and the vietoris-rips complex, .
- M. Adamaszek, F. Frick and A. Vakili, On homotopy types of Euclidean Rips complexes,
 Discrete Comput. Geom. 58 (2017) 526.
- 17. K. Borsuk, *Theory of retracts*, Monografie Matematyczne, Tom 44 (Państwowe Wydawnictwo
 Naukowe, Warsaw, 1967).
- 18. A. Dold, Lectures on algebraic topology, Classics in Mathematics (Springer-Verlag, Berlin,
 1995), reprint of the 1972 edition.
- 19. J.-C. Hausmann, On the Vietoris-Rips Complexes and a Cohomology Theory for Metric Spaces,
 in *Prospects in Topology (AM-138)*, ed. F. Quinn (Princeton University Press, 1995), Proceedings of a Conference in Honor of William Browder. (AM-138), pp. 175–188.
- 729 20. F. Lecci, A. Rinaldo and L. Wasserman, Statistical analysis of metric graph reconstruction, J.
 730 Mach. Learn. Res. 15 (2014) 3425.
- D. Burago, Y. Burago and S. Ivanov, A Course in Metric Geometry, Crm Proceedings & Lecture Notes (American Mathematical Society, 2001).
- 22. M. Gromov, J. Lafontaine and P. Pansu, Metric Structures for Riemannian and Non-Riemannian Spaces, Progress in Mathematics Birkhäuser (Birkhäuser, 1999).
- 23. D. N. Kozlov, Combinatorial algebraic topology, number v. 21 in Algorithms and computation in mathematics (Springer).
- 24. J. R. Munkres, Elements Of Algebraic Topology (Addison-Wesley Publishing Company, 1996),
 Second edition.
- 739 25. E. H. Spanier, Algebraic topology, volume 55 (Springer Science & Business Media, 1994).
- 740 26. M. Gromov, Homotopical effects of dilatation, J. Differential Geom. 13 (1978) 303.
- 741 27. M. Gromov, Filling Riemannian manifolds, J. Differential Geom. 18 (1983) 1.
- Z8. J. M. Sullivan, Discrete Differential Geometry (Birkhäuser Verlag AG, Basel, Switzerland, 2008), ch. Curves of Finite Total Curvature, pp. 137–161, edited by A. Bobenko, P. Schröder, J.M. Sullivan, and G.M. Ziegler.
- 745
 29. P. Alexandroff, Über den allgemeinen Dimensionsbegriff und seine Beziehungen zur elementaren
 746 geometrischen Anschauung, Mathematische Annalen 98 (1928) 617.
- ⁷⁴⁷ 30. J. R. Munkres, *Topology*, Featured Titles for Topology Series (Prentice Hall, Incorporated,

- $26\quad \textit{Fasy, Komendarczyk, Majhi, and Wenk}$
- 748 2000).
- 749 31. E. W. Chambers, V. de Silva, J. Erickson and R. Ghrist, Vietoris–Rips complexes of planar point sets, *Discrete & Computational Geometry* **44** (2010) 75.
- ⁷⁵¹ 32. A. Hatcher, Algebraic Topology (Cambridge University Press, 2002), First edition.